REGULAR ARTICLE

Polymer Journal

Molecular Aggregation State of Surface-grafted Poly{2-(perfluorooctyl)ethyl acrylate} Thin Film Analyzed by Grazing Incidence X-ray Diffraction

By Hiroki YAMAGUCHI,[1] *Koji HONDA,*[1] *Motoyasu KOBAYASHI,*[2] *Masamichi MORITA,*[3] *Hiroyasu MASUNAGA,*[4] *Osami SAKATA,*[4] *Sono SASAKI,*[4,5] *and Atsushi TAKAHARA*[1,2,5,*]

Surface-initiated atom transfer radical polymerization of 2-(perfluorooctyl)ethyl acrylate on a flat silicon wafer was carried out to give poly{2-(perfluorooctyl)ethyl acrylate} (PFA-C_8) brush thin film with three different thicknesses of 4, 11, and 43 nm, respectively. The water contact angle of the PFA-C_8 brush surface was 120°. The molecular aggregation state of the perfluoroalkyl (R_f) group of PFA-C_8 brush was analyzed by X-ray reflectivity (XR), wide-angle X-ray diffraction, and grazing incidence X-ray diffraction (GIXD) measurements. XR analysis revealed that R_f groups at the air/brush interface formed a densely packed structure, while a relatively low-density region was generated at the brush/substrate interface. The peaks of in-plane GIXD for brush films with thicknesses of 11 and 43 nm were observed at $q_{xy} = 12.5\,nm^{-1}$, which indicated that R_f groups at the outermost surface oriented perpendicular to the surface of silicon substrate. In an out-of-plane diffraction profile of the 43 nm-thick PFA-C_8 brush film, peaks corresponding to a periodic length of the bilayer lamellae were observed. Therefore, R_f groups of the thicker brush film were crystallized and formed ordered bilayer lamellar structure at the outermost surface. In contrast, no diffraction pattern was observed from the PFA-C_8 at a thickness of 4 nm by WAXD and GIXD. These results indicate that an amorphous layer was formed at the interface of the brush/substrate. The R_f groups at the anchoring region of the brush could not form a sufficiently ordered structure due to immobilization of brush chain ends on the substrate. It was suggested that the R_f groups in a PFA-C_8 brush thin film at the outermost surface aggregated in a different manner from those in the anchoring region.

KEY WORDS: Perfluoroalkyl Acrylate / Polymer Brush / Water-Repellant Surface / X-Ray Reflectivity / Grazing Incidence X-ray Diffraction / Surface-initiated Polymerization /

It has been well-known that polymers with perfluoroalkyl (R_f) groups show excellent chemical and thermal stability, non-adhesive properties, low friction coefficients, low surface free energy, and antifouling behavior. These properties of fluorinated polymers are primarily caused by unique C-F bonds which have a large binding energy and quite a low dielectric constant due to short bonding distance between carbon and fluorine atom with high electro negativity. However, the surface component, orientation packing, and end groups also affect the surface behavior of the polymer films.[1–3] When the surface is uniformly covered with trifluoromethyl (CF_3) groups,[4] excellent water repellency and a very low energy surface can be achieved.[5] In the case of poly(fluoroalkyl acrylate)s with long R_f groups, the molecular aggregation state of the R_f groups at the side chains affects the surface wettablity.[6,7]

We have recently reported the relationship between the molecular aggregation states and the water repellency of poly(perfluoroalkyl acrylate) (PFA-C_y, where y is the number of fluoromethylene in the R_f unit) thin films prepared by spin-coating of various types of PFA-C_y on silicon wafer.[8] PFA-C_y with shorter R_f chains ($y \leq 6$) afford relatively low receding contact angles of water droplets, whereas those with longer R_f chains ($y \geq 8$) show larger contact angles. Wide-angle X-ray diffraction (WAXD) in the symmetric reflection geometry revealed that PFA-C_y with $y \geq 8$ was crystallized and formed ordered bilayer lamellar structures of R_f groups. The molecular aggregation structure of PFA-C_y thin films at the surface region was characterized by in-plane and out-of-plane grazing incidence X-ray diffraction (GIXD).[9] In-plane diffractions corresponding to the hexagonal packing of the R_f groups were observed for PFA-C_y with $y \geq 8$ at the surface and bulk regions. In contrast, out-of-plane diffraction gave only peaks corresponding to the bilayer lamellar structure. These results suggest that the water repellent mechanism of PFA-C_y can be attributed to the presence of highly ordered R_f chains at the air/polymer interface.[10,11] We found that the stable water repellency of PFA-C_y with $y \geq 8$ originated from its surface ordering and the perpendicular orientation of R_f groups against the film surface.

Unfortunately, the physical adhesion of spin-cast film to the substrate is relatively weak because the interaction between the

[1]Graduate School of Engineering, Kyushu University, 744 Motooka, Nishi-ku, Fukuoka 819-0395, Japan
[2]Institute of Materials Chemistry and Engineering, Kyushu University, 744 Motooka, Nishi-ku, Fukuoka 819-0395, Japan
[3]Daikin Industries Ltd, 1-33 Nishihitotsuya, Settsu 566-0044, Japan
[4]Japan Synchrotron Research Institute, Mikazuki Sayo 671-5198, Japan
[5]The RIKEN Harima Institute, Mikazuki Sayo 671-5198, Japan
*To whom correspondence should be addressed (Tel: +81-92-802-2517, Fax: +81-92-802-2518, E-mail: takahara@cstf.kyushu-u.ac.jp).

 doi:10.1295/polymj.PJ2008107

fluoropolymer and the solid surface is based only on van der Waals forces. One possible method to overcome this weak adhesion is the immobilization of fluorinated polymer onto the substrate. Actually, spin-cast films are easily scratched out by friction or rubbing, though the tethered polymer surface shows good wear resistance[12] because the polymer chain ends are covalently bound with substrate. Polymer chains tethered to a surface or interface with a sufficiently high grafting density are referred to as "polymer brush."[13] Normally, polymer brushes are prepared by chemisorption of polymers with reactive functional groups onto the solid surface ("grafting-to" method) or by surface-initiated polymerization of monomers from initiator-immobilized substrate ("grafting-from" method). Tsubokawa *et al.* have immobilized a surface initiator with a 4,4-azobis(4-cyanopentanoic acid) moiety on a glass plate to initiate polymerization of perfluorohexylethyl acrylate from the surface.[14] Rühe and his co-workers have prepared poly{2-(perfluorooctyl)ethyl acrylate} (PFA-C_8) brush by surface-initiated thermal radical polymerization from the porous silica immobilized with an azo-type surface initiator to give a super liquid-repellent surface.[15] Over the last decade, high-density and well-defined polymer brushes have been readily synthesized, since controlled polymerization techniques have been exploited for surface-initiated polymerization. Atom transfer radical polymerization (ATRP), which is a type of the living radical polymerization, has been widely employed for the formation of polymer brushes because ATRP is compatible with various functionalized monomers. As a result, various tailored fluoropolymer brushes have been prepared by surface-initiated polymerization. Ma *et al.* have prepared poly{2-(perfluorooctyl)ethyl methacrylate} brush on cross-linked polydimethylsiloxane containing the alkylbromide moiety to give a stable hydrophobic surface.[16] Diblock copolymer consisting of poly(methyl acrylate)-*block*-poly(pentafluoro acrylate) has also been prepared by surface-initiated ATRP from porous silica immobilized with alkyl bromide.[17] The solvent repellency of the porous silica surface was improved by grafting of fluoropolymers. The influence of the branching structure of polymer brush on surface wettablity was investigated by Kang *et al.*, who prepared branched fluoropolymer brush using 2,3,4,5,6-pentafluorostyrene (PFS) and 4-vinylbenzyl chloride as an inimer.[18] They reported that the water contact angle depends on the composition of the fluoropolymer block and inimer, and that the surface roughness is caused by the branching structure of the brush. Surface rearrangement properties upon solvent and thermal treatment were observed on polystyrene-*block*-PFA-C_8 and polystyrene-*block*-poly(PFS) brushes.[19] A similar result has also been observed on the poly(2,2,2-trifluoroethyl methacrylate)-*block*-polyacrylamide brush surface on flat silicon wafer by Wang *et al.*[20] Tsukruk *et al.* prepared thick (50–90 nm) poly(styrene-*co*-PFS) brush to investigate the thermal and mechanical properties of the brush surface by AFM-based techniques using a thermal probe.[21]

In this paper, we prepared the PFA-C_8 brush thin films with a thickness of 4–50 nm by surface-initiated ATRP to analyze the molecular aggregation states of PFA-C_8 brush thin films with R_f groups by contact angle measurements, WAXD, X-ray reflectivity (XR), and in-plane and out-of plane GIXD. This research will demonstrate the relationship between the brush thickness and the molecular aggregation state of R_f groups to show the gradient structure along with the distance from the outermost brush surface to the migrated substrate interface.

EXPERIMENTAL

Materials

Copper(I) bromide (CuBr, Wako Pure Chemicals, 98%) was purified by washing with acetic acid and ethanol and was dried under vacuum. Ethyl 2-bromoisobutylate (EB) (TCI, 99%) and 4,4′-dinonyl-2,2′bipyridyl (Aldrich) were used as received. Surface initiator, (2-bromo-2-methyl)propionyloxyhexyltriethoxysilane (BHE),[22] was synthesized by hydrosilylation of 5-hexenyl 2-bromoisobutylate treated with triethoxysilane using the Karstedt catalyst.[23] FA-C_8 monomer (Daikin Industry Ltd.) was purified by repeated distillation under reduced pressure to remove other types of monomers such as 2-(perfluorodecyl)ethyl acrylate. The purify of FA-C_8 was over 98% by gas chromatography. Water for the contact angle measurement was purified with the NanoPure Water system (Millipore, Inc.).

Initiator-immobilized Silicon Substrate

The discotic silicon (111) wafers (diameter = 1 inch, thickness = 0.3 mm) were cleaned by washing with piranha solution ($H_2SO_4/H_2O_2 = 7/3$, v/v) at 373 K for 1 h and by exposure to vacuum ultraviolet-ray (VUV, $\lambda = 172$ nm) for 10 min under reduced pressure (30 Pa). Surface-initiator BHE was immobilized on a purified silicon wafer by the chemical vapor adsorption method to form a monolayer as reported previously.[24,25] BHE-immobilized silicon wafers were rinsed with HPLC-grade ethanol and were dried *in vacuo* at room temperature for 1 h and stored in a dark place. The surface chemical composition of brush film was analyzed by X-ray photoelectron spectroscopy (XPS) and Fourier transform infrared (FT-IR) measurements.

General Procedure for Surface-initiated ATRP of FA-C_8

A typical surface-initiated ATRP of FA-C_8 was performed as follows (Scheme 1). A few sheets of the initiator-immobilized silicon wafers, CuBr (0.075 mmol), and 4,4′-dinonyl-2,2′-bipyridyl (0.150 mmol), were introduced into a glass vessel with a stop cock and were dried by repeating a degas and argon purge. FA-C_8 monomer (31.7 mmol), and EB (0.075 mmol) were added to the catalyst. Oxygen was removed by the freeze-pump-thaw cycles. The polymerization reaction was conducted at 383 K for 72 h under argon to simultaneously generate PFA-C_8 brush from the silicon substrate and free PFA-C_8 from EB. The reaction was quenched by opening the glass vessel to air at 273 K. The reaction mixture was diluted with AK-225 (Asahi Glass Co.), which is a mixture of 1,1-dichloro-2,2,3,3,3-pentafluoropropane and 1,3-dichloro-1,1,2,2,3-pentafluoropropane, and poured into THF to precipitate the free polymer. The

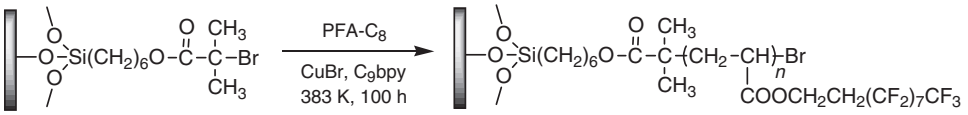

Scheme 1. Preparation of PFA-C_8 brush by surface-initiated ATRP.

silicon wafers were washed with AK-225 using a Soxhlet apparatus for 8 h to remove the free polymer absorbed on their surface, and were dried under reduced pressure at 373 K for 1 h. All samples were annealed at 373 K for 1 h and gradually cooled to room temperature at 10 K/min.

Measurements

The number-average molecular weights (M_n) and molecular weight distribution (MWD) of the free polymer were determined by size-exclusion chromatography (SEC) recorded on a JASCO instrument equipped with a JASCO 2031plus RI detection, which runs through two directly connected polystyrene gel columns (TSK gel SuperHM-M, 0.6 mL/min) using 1,1,1,3,3,3-hexafluoro-2-propanol (HFIP) as an eluent at 313 K. A calibration curve was constructed from a series of PMMA standards.

The thicknesses of the polymer brush and the spin-coat film on the silicon substrate were determined by imaging ellipsometer (Nippon Laser & Electronics Lab.) equipped with a YAG laser (532.8 nm). The polarizer angle was fixed at 50°, and a refractive index 1.36 was assumed for the calculations of the film thickness. The FT-IR spectra were recorded on a Spectrum One KY type (PerkinElmer. Inc.) system coupled with a Mercury-Cadmium-Tellurium (MCT) detector. The incident angle of the *p*-polarized infrared beam was 73.7° (Brewster angle) in order to eliminate the multiple reflection of the infrared beam within the silicon wafer substrate.[26,27] As substrates for the FT-IR measurements, silicon wafers with both surfaces polished were used to reduce the influence of fringes in the spectra. For IR spectra, 1024 scans were collected with a resolution of 0.5 cm^{-1}.

Atomic force microscopic (AFM) observations were carried out by the SPA 400 with an SPI 3800N controller (SII Nano Technology Inc.) in air at room temperature, using a Si_3N_4 integrated tip on a commercial triangle 200-μm cantilever (Olympus Co., Ltd) with a spring constant of 0.09 N/m. The contact angles against water, hexadecane, and methylene iodide (each droplet volume were 2 μL) were recorded with a drop shape analysis system DSA 10 Mk2 (KRÜSS Inc.) equipped with a video camera. In an inclinable plane, a sample on a stage was tilted until a 50-μL water droplet began to slide down on to the sample surface. Subsequently, the advancing contact angle (θ_A), receding contact angle (θ_R), and sliding angle (θ_S) were determined. XPS measurements were carried out on an XPS-APEX (ULVAC PHI Inc.) at 10^{-5} Pa using a monochromatic Al-K_α X-ray source at a photoelectron with a take-off angles of 45°.

The wide-angle X-ray diffraction (WAXD) measurements were carried out on a Rigaku RINT 2500V (Rigaku Corp.) with a Cu-K_α X-ray source (40 kV, 200 mA) for PFA-C_8 brush thin films. The wavelength, λ, of the incident X-ray was 0.1542 nm. The data-collection time was 3 s per step at 0.05° intervals. WAXD measurements were carried out by symmetrical reflection geometry. In this method, Bragg diffraction from crystallographic planes parallel to the substrate is obtained from bulk regions. The scattering vector, q, in specular reflectivity is defined by $q = (4\pi/\lambda)\sin\theta$, where λ and θ are the wavelength and incident angle of the X-ray beam from the horizontal position, respectively. The X-ray reflectivity (XR) and grazing incidence X-ray diffraction (GIXD) measurements were carried out on a BL-13XU beam line of SPring-8 (Japan Synchrotron Radiation Research Institute, Hyogo, Japan) using an incident X-ray with a wavelength λ of 0.100 nm.[28] The data collection time was 3.0 s per step at 0.1° intervals. The incident and reflection angles of XR measurements were kept at same magnitude for a specular condition. Model calculations and data analysis for the XR were carried out using scientific software, XRR, a program provided by Rigaku Corp. The procedure for data fitting and simulation was also based on Parratt's algorithm[29] and the theory of Sinha *et al.*[30] In the GIXD measurement, a strong diffraction was observed on the ultrathin films when the incident angle (α_i) to the sample was below a critical angle (α_c). Under this condition, the X-ray underwent total external reflection and penetrated the sample as evanescent waves. The α_c of organosilane was *ca.* 0.15°. Bragg diffractions from crystallographic planes perpendicular to the substrate were obtained from the surface and bulk regions at α_i of 0.08 and 0.16, respectively.[31] Diffractions from the sample were detected in the in-plane and out-of-plane direction by a scintillation counter. The sample cell was wrapped with a polyimide (KAPTON™) dome, which was blown up by helium gas to prevent the oxidation of sample during the GIXD measurements. The data obtained were corrected for background and then analyzed. The GIXD profiles were fitted using a Lorentzian function on a linear background. All XR and GIXD observations were carried out at room temperature.

RESULTS AND DISSCUSION

Surface-initiated ATRP of PFA-C_8 Brush Thin Films on a Silicon Wafer

Surface-initiated ATRP of FA-C_8 was carried out from the BHE–immobilized silicon wafer in the presence of EB as a free initiator coupled with CuBr and 4,4′-dinonyl-2,2′-bipyridyl at 383 K. The M_n of PFA-C_8 brushes on silicon wafer and simultaneously obtained unbound polymer were expected to be same.[32–36] The M_n of the corresponding free polymer were estimated to be approximately 14,000–30,000 by PMMA-

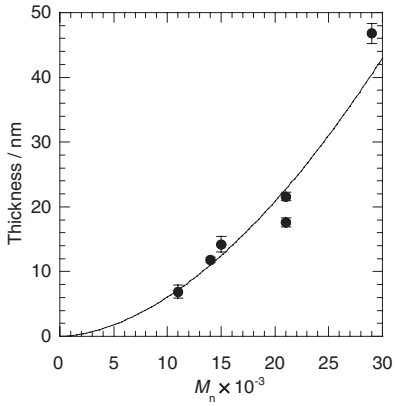

Figure 1. Relationship between number-average molecular weights and thickness.

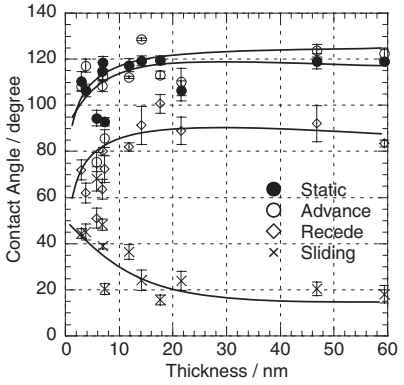

Figure 2. Relationship between thickness and contact angles.

Table I. Water contact angles and surface free energies of PFA-C_8 brush films

	M_n [a]	Thickness[b] nm	Water contact angle, degree				Surface Free Energy, γ_{sv} [e] mN/m
			Static θ [c]	θ_A [d]	θ_R [d]	θ_S [d]	
Sample 1	18 k	4	107	117	62	45	13.4
Sample 2	14 k	12	117	112	82	37	12.9
Sample 3	29 k	43	119	124	92	21	11.5

a SEC in HFIP at 313 K using PMMA standards. *b* Ellipsometry. *c* 2 μL. *d* 50 μL. *e* Determined by Orwen's equation using static contact angle of CH_2I_2.

standard calibration on a SEC using HFIP as an eluent. The relationship between M_n and the thickness of the brush are shown in Figure 1. The thickness of the polymer brush was determined to be *ca.* 4–50 nm by ellipsometer. In general, the thickness of densely-grafted polymer brush increases linearly with the M_n of the polymer because chains are stretched away from the surface in order to avoid overlap of each polymer chain. According to the proportional relationship between the thickness and M_n of polymers, the graft density was estimated to be *ca.* 0.15 chains/nm^2 if the refractive index was isotropic in the brush thin layer. Considering a molecular size of FA-C_8, graft density of 0.15 chains/nm^2 is high enough to form a brush structure. The brushes with lower graft densities, such as sample 1 in Table I, were also occasionally obtained probably due to the technical trouble in the polymerization process; however, almost all brushes had higher grafting densities than 0.1 chains/nm^2. AFM observations revealed that a homogeneous polymer layer was formed on the substrate, and that the surface roughness was 0.8–1.5 nm in a dry state in the $5 \times 5\,\mu m^2$ scanning area. As mentioned above, various types of fluoropolymer brushes have already been prepared by other researcher groups but the brush thicknesses have been less than 20 nm. In the present, however, we successfully prepared homo PFA-C_8 brush film thicker than 50 nm by surface-initiated ATRP.

The water repellency of the PFA-C_8 brush surface can be seen in the contact angle of the water droplet. Figure 2 represents the dependence of the water static contact angle of water on the thickness of the PFA-C_8 brush. The static contact angles of all brush samples were found to be above 90°. When increasing the brush thickness from 4 to 20 nm, the contact angle gradually increased, finally static 120°, which corresponds to the contact angle of spin cast film. Similar trends were also observed in advancing, receding, and sliding angles. The surface free energies for PFA-C_8 brush thin films, which were estimated by Owens and Wendt's equation[37] based on the static contact angles of water and methylene iodide, slightly decreased from 13.4 mN/m to 11.5 mN/m with increasing brush thickness from 4 to 43 nm. Dynamic contact angles and surface free energy of the typical brush sample are summarized in Table I. The contact angle hysteresis, which is expressed as $\theta_A - \theta_R$, of a water droplet on PFA-C_8 brush film depended on the brush thickness. A water droplet on thicker brush film such as sample 3 began to slide, maintaining high θ_A and θ_R, when the film was tilted to $\theta_S = 21°$, while a sliding water droplet on thin brush film such as sample 1 formed an asymmetric shape with high θ_A and low θ_R. We suppose that these different wetting behaviors were caused by the difference in ordered structures of the R_f groups of PFA-C_8 brush film, as described in a later section.

X-Ray Reflectivity

The specular reflectivity of X-rays provides information regarding electron-density variations normal to the surface with angstrom resolution. Figure 3(a) show a reflectivity profile of PFA-C_8 brush film with 11 nm thick, and corresponding fit which was calculated by the density distribution of the thin film as shown in Figure 3(b). The thickness of the brush film can be roughly estimated intervals of the Kiessig fringes in the XR curve as well as on ellipsometry. The profile of XR curve,

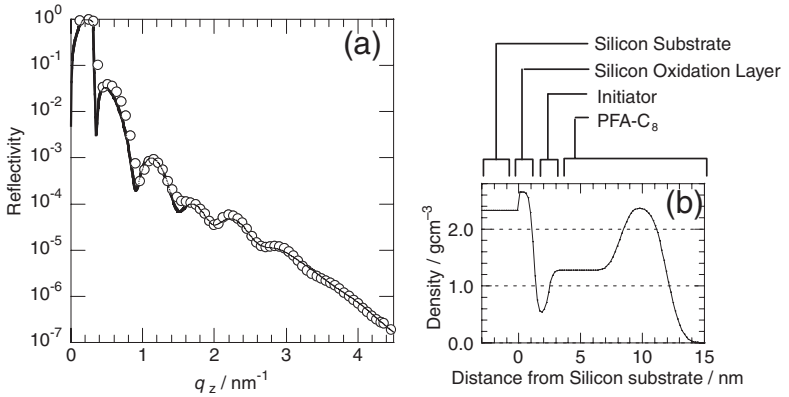

Figure 3. XR profiles of PFA-C_8 brush with a thickness of 11 nm thick and the fitting curve calculated by XRR software in the Figure 3(a). The assumed density profile is shown in the Figure 3(b).

however, seems to overlap with some of Bragg diffraction peaks. This film basically consists of 4 layer, a silicon substrate, a SiO_2 layer, surface initiator layer, and a PFA-C_8 brush layer, but the best fitting curve required five layers. The bulk density of silicon and SiO_2 are 2.33 and 2.65 g·cm^{-3}, respectively. As can be seen from Figure 3(b), the bulk density inside the brush layer near the tethered point at the silicon substrate was relatively low, and the density gradually increased along with the distance from the substrate. The outermost area facing air revealed the highest density as 2.3 g cm^{-3}, which is close value to the density of poly(tetrafluoroethylene) (PTFE). The fitting curve corresponds perfectly to the XR profile, which was fitted by XRR software using step functions. This density distribution indicates that R_f groups at the side chains aggregate with each other to form the same assembled structure on the outermost surface. A similar result was obtained in the XR profile for the PFA-C_8 brush thin films with 43 nm thick. Bragg diffraction peak at $q_z = 2.0$ and 4.0 nm^{-1} were observed in XR curve, although the result of XR profile not shown in this paper. Thus, the density distribution of the PFA-C_8 brush thin film is not homogeneous. In other words, molecular chains seem to aggregate to the outermost surface of PFA-C_8 thin films.

Wide Angle X-ray Diffraction of PFA-C_8 Brush

Symmetric WAXD profiles of PFA-C_8 brush thin films with thicknesses of 4 nm, 11 nm, and 43 nm and unmodified silicon wafer are shown in Figure 4. The largest peak at $q_z = 20$ nm^{-1} corresponds to the silicon crystal in the substrate. Although neither of sample 1 nor 2 showed a peak except for silicon wafer, sample 3 with its thickness of 43 nm had a diffraction peak at $q_z = 3.84$ nm^{-1}. The side-chain R_f length and the layer spacings calculated from the X-ray diffraction patterns are 1.6 and 3.1 nm, respectively. The layer spacings are approximately twice as long as the side-chain lengths. In the previous study of PFA-C_8 thin films prepared by the spin-cast method, the same diffraction peak was observed at $q_z = 1$–7 nm^{-1}, which is assignable to a high-order diffraction pattern due to the lamellar structure of the R_f groups. In the case of this scattering geometry, Bragg diffraction from the crystallographic plane parallel to the substrate is obtained from bulk regions, indicating that the lamellar structure is oriented parallel to the substrate and that R_f groups are oriented almost perpendicular to the substrate.

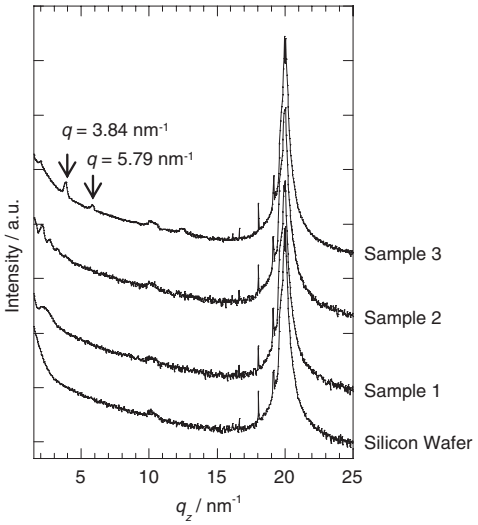

Figure 4. Symmetric WAXD profiles of PFA-C_8 brushes with thicknesses of 4, 11, and 43 nm.

Grazing-incidence X-ray Diffraction of PFA-C_8 Brush

Figure 5 shows the in-plane GIXD profiles measured at 0.08° for PFA-C_8 brush films with thicknesses of 4, 11, and 43 nm. Sharp and strong peaks were appeared for PFA-C_8 brush thin films with thickness of 11 and 43 nm at *ca.* 12.6 nm^{-1}. Hence, the side chains of the polymers are oriented normal to the surface. The *d*-spacing calculated from the peak position was *ca.* 0.50 nm, which was close to the intermolecular distance between helical chains of PTFE hexagonal (d = 0.49 nm)[38–41] and was almost the same as the intermolecular distance between R_f groups at the side chains of PFA-C_8 spin cast films (d = 0.50 nm). Therefore, it was suggested that the rigid rod-like R_f groups underwent hexagonal packing in the brush films of PFA-C_8 with thicknesses of 11 and 43 nm.

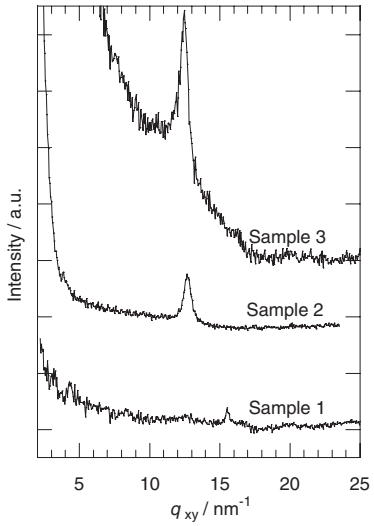

Figure 5. In-plane GIXD profiles of PFA-C_8 brush thin films with thicknesses of 4, 11, 43 nm.

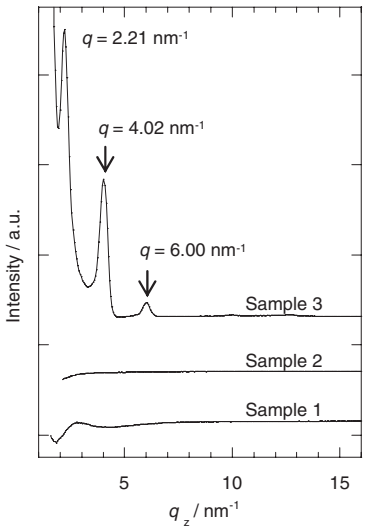

Figure 6. Out-of-plane GIXD profiles of PFA-C_8 brush thin films with thicknesses of 4, 11, 43 nm.

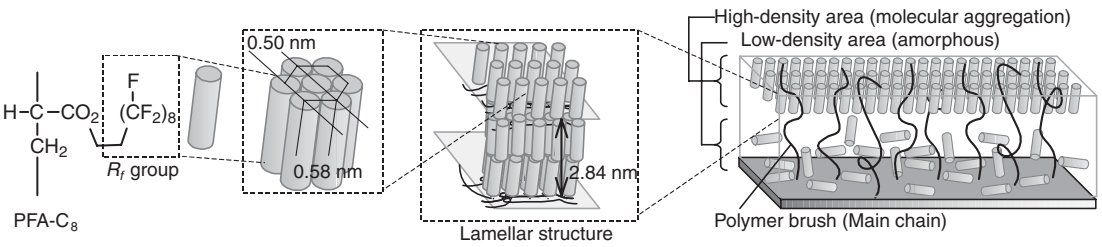

Figure 7. Schematic image of the molecular aggregation structure of R_f groups attached to PFA-C_8 brush. The R_f group at the side chain of PFA-C_8 brush is represented as a small "rod" in this illustration.

However, the d-spacing of PFA-C_8 brush films was slightly larger than that of PTFE ($d = 0.49$ nm) and PFA-C_8 spin cast film ($d = 0.50$ nm), indicating that orthorhombic hexagonal packing of R_f groups were oriented almost perpendicular to the silicon wafer. On the other hand, the PFA-C_8 brush thin film with thickness of 4 nm (sample 1) had no peak around $q_{xy} = 12$–$14\,\mathrm{nm}^{-1}$ in the profile. Although a small peak was appeared at $q_{xy} = 15.5\,\mathrm{nm}^{-1}$, it was regarded as a noise because it was not reproducible in our in-plane GIXD measurements.

Figure 6 represents the out-of-plane GIXD profiles of samples 1, 2, and 3. PFA-C_8 brush film with a thickness of 43 nm clearly showed strong diffraction peaks at $q_z = 2.21$, 4.02, and $6.00\,\mathrm{nm}^{-1}$, corresponding to the d-spacings of *ca.* 2.84, 1.56, and 1.05 nm, respectively. These peaks are assignable to the lamellar structure of R_f group. These Bragg diffractions indicate that the (*001*) crystallographic planes are parallel to the substrate. These d-spacings of PFA-C_8 brush thin film were completely close to that of PFA-C_8 spin-coat films. In contrast, no peaks appeared in the profiles of samples 1 and 2 with 4 and 11 nm thick. We supposed that the R_f groups in brushes thinner film than 11 nm could not form sufficient lamellar structures, thus resulting in the absence of diffraction peak in GIXD profile.

Aggregation Structure of PFA-C_8 Brush Thin Films

Considering these X-ray diffraction patterns, the R_f aggregation states seemed to depend strongly on the brush thickness. A thicker brush film such as that in sample 3 showed a strong diffraction pattern in the symmetric WAXD, and the in-plane and out-of-plane GIXD; therefore, R_f groups undergo hexagonal packing on the outermost surface and are oriented almost perpendicular to the substrate. Moreover, R_f groups fabricate a lamellar structure, that is oriented parallel to the surface. In contrast, R_f groups closely located around the substrate in the present study could not diffuse sufficiently to form an aggregate structure because the conformation of the main chain was restricted by covalent bonding with the substrate. As a result, an amorphous structure with low density formed at the substrate interface in the brush layer, but no crystalline structure was fabricated on the thin brush film such as that in sample 1. Similar low crystallization behavior was also observed in poly(vinyl alcohol) brush thin film.[42] Figure 7 provides a schematic representation of the molecular aggregation structure of R_f groups speculated from XR and GIXD profiles. We supposed that these highly rigid and ordered structures of the R_f groups on the outermost surface created a surface with higher water repellency. In the case of brush films thinner than 10 nm, the smaller contact angles and large

hysteresis ($\theta_A - \theta_R$) must be caused by amorphous orientation of the R_f groups attached to brush chains, of which molecular motion was restricted by the tethered structure on the substrate.

CONCLUSION

Surface-initiated ATRP of FA-C_8 produced PFA-C_8 brush thin films with a thickness of 4–50 nm thick on silicon substrate. This is the first report of the synthesis of homo PFA-C_8 brush thicker than 50 nm. Higher hydrophobicity and water repellency was observed on the surface of the thicker PFA-C_8 brush films. A combination of XR and GIXD analysis of PFA-C_8 brush film showed the different aggregation state of the R_f groups at the air/brush interface and the substrate/brush interface. On the outermost surface, R_f groups at the side chains formed a hexagonal packing structure due to the low surface free energy, and were oriented almost perpendicular to the substrate to result in a lamellar structure and a high-density area. On the other hand, the conformation and molecular motion of polymer chains at the brush/substrate interface were restricted by anchoring bonds to prevent the ordered structure formation of R_f groups, producing an amorphous layer with low density. A similar anchoring effect can be applied to thinner brush film, in which R_f groups can't achieve sufficient ordered aggregation or form a lamellar structure, thus resulting in an amorphous R_f orientation with lower water repellency.

Acknowledgment. The present work is supported by a Grant-in-Aid for the Global COE Program, "Science for Future Molecular Systems," and partially supported by a Grant-in Aid for Young Scientist (B) (19750098) from the Ministry of Education, Culture, Science, Sports and Technology of Japan. The synchrotron radiation X-ray diffraction experiments were performed at SPring-8 with the approval of Japan Synchrotron Radiation Research Institute (JASRI).

Received: May 2, 2008
Accepted: June 5, 2008
Published: July 24, 2008

REFERENCES

1. A. G., Pittman, in "Fluoropolymers," L. A. Wall, Ed., Wiley-Interscience, New York, 1972, p419.
2. H. Yokoyama, K. Tanaka, A. Takahara, T. Kajiyama, K. Sugiyama, and A. Hirao, *Macromolecules*, **37**, 939 (2004).
3. M. Hikita, T. Nakamura, K. Tanaka, A. Takahara, and T. Kajiyama, *Langmuir*, **20**, 5304 (2004).
4. E. F. Hare, E. G. Shafrin, and W. A. Zisman, *J. Phys. Chem.*, **58**, 236 (1954).
5. T. Nishino, M. Meguro, K. Nakamae, M. Matsushita, and Y. Ueda, *Langmuir*, **15**, 4321 (1999).
6. Y. Katano, H. Tomono, and T. Nakajima, *Macromolecules*, **27**, 2342 (1994).
7. V. V. Volkov, N. A. Platé, A. Takahara, T. Kajiyama, N. Amaya, and Y. Murata, *Polymer*, **33**, 1316 (1992).
8. K. Honda, M. Morita, H. Otsuka, and A. Takahara, *Macromolecules*, **38**, 5699 (2005).
9. K. Honda, H. Yakabe, T. Koga, S. Sasaki, O. Sakata, H. Otsuka, and A. Takahara, *Chem. Lett.*, **34**, 1024 (2005).
10. K. Honda, H. Yamaguchi, M. Kobayashi, M. Morita, and A. Takahara, *J. Phys. Conf. Ser.*, **100**, 012035 (2008).
11. K. Honda, M. Morita, and A. Takahara, *Koubunshi Ronbunshu*, **64**, 181 (2007).
12. H. Sakata, M. Kobayashi, H. Otsuka, and A. Takahara, *Polym. J.*, **37**, 767 (2005).
13. Polymer Brushes: Synthesis, Characterization, Applications, R. C. Advincula, W. J. Brittain, K. C. Caster, and J. Ruhe, Ed., Wiley VCH, Weinheim 2004.
14. N. Tsubokawa and M. Satoh, *J. Appl. Polym. Sci.*, **65**, 2165 (1997).
15. D.-H. Jung, I. J. Park, Y. K. Choi, S.-B. Leel, H. S. Park, and J. Rühe, *Langmuir*, **18**, 6133 (2002).
16. Y. Wu, Y. Huang, and H. Ma, *J. Am. Chem. Soc.*, **129**, 7226 (2007).
17. A. M. Granville and W. J. Brittain, *Macromol. Rapid. Commun.*, **25**, 1298 (2004).
18. F. J. Xu, Z. L. Yuan, E. T. Kang, and K. G. Neoh, *Langmuir*, **20**, 8200 (2004).
19. A. M. Granville, S. G. Boyes, B. Akgun, N. D. Foster, and W. J. Brittain, *Macromolcules*, **37**, 2790 (2004).
20. Y. Xu, H. Li, Y. Li, D. Wang, Y. Song, and J. Wang, *Polym. Prepr. (Am. Chem. Soc., Div. Polym. Chem.)*, **47(2)**, 1198 (2006).
21. M. Lemieux, S. Minko, D. Usov, M. Stamm, and V. V. Tsukruk, *Langmuir*, **19**, 6126 (2003).
22. K. Ohno, T. Morinaga, K. Koh, Y. Tsujii, and T. Fukuda, *Macromolecules*, **38**, 2137 (2005).
23. M. Kobayashi and A. Takahara, *Chem. Lett.*, **34**, 1582 (2005).
24. H. Tada and H. Nagatama, *Langmuir*, **10**, 1472 (1994).
25. M. Kobayashi, Y. Terayama, N. Hosaka, M. Kaido, A. Suzuki, N. Yamada, N. Torikai, K. Ishihara, and A. Takahara, *Soft Matter* **3**, 740 (2007).
26. R. Maoz, J. Sagiv, D. Degenhardt, H. Möhwald, and P. Quint, *Supramol. Sci.*, **2**, 9 (1995).
27. K. Kojio, S.-R. Ge, A. Takahara, and T. Kajiyama, *Langmuir* **14**, 971 (1998).
28. O. Sakata, Y. Furukawa, S. Goto, T. Mochizuki, T. Uruga, K. Takeshita, H. Ohashi, T. Ohata, T. Matsushita, S. Takahashi, H. Tajiri, T. Ishikawa, M. Nakamura, M. Ito, K. Sumitani, T. Takahashi, T. Shimura, A. Saito, and M. Takahashi, *Surf. Rev. Lett.*, **10**, 543 (2003).
29. L. G. Parratt, *Phys. Rev.*, **95**, 359 (1954).
30. S. K. Sinha, E. B. Sirota, S. Garoff, and H. B. Stanley, *Phys. Rev. B*, **38**, 2297 (1988).
31. T. P. Russell, *Mater. Sci. Rep.*, **5**, 171 (1990).
32. T. von Werne and T. E. Patten, *J. Am. Chem. Soc.*, **121**, 7409 (1999).
33. M. Husseman, E. E. Malmstrom, M. McNamura, M. Mate, D. Mecerreyes, D. G. Benoit, J. L. Hedrick, P. Mansky, E. Huang, T. P. Russell, and C. J. Hawker, *Macromolecules*, **32**, 1424 (1999).
34. J. Pyun, S. Jia, T. Kowalewski, G. D. Patterson, and K. Matyjaszewski, *Macromolecules*, **36**, 5094 (2003).
35. R. Matsuno, K. Yamamoto, H. Otsuka, and A. Takahara, *Macromolecules*, **37**, 2203 (2004).
36. S. Blomberg, S. Ostberg, E. Harth, A. W. Bosman, B. van Horn, and C. J. Hawker, *J. Polym. Sci., Part A: Polym. Chem.*, **40**, 1309 (2002).
37. D. K. Owens and R. C. Wendt, *J. Appl. Polym. Sci.*, **13**, 1741 (1969).
38. C. W. Bunn and E. R. Howells, *Nature*, **174**, 549 (1954).
39. J. M. Corpart, S. Girault, and D. Juhué, *Langmuir*, **17**, 7237 (2001).
40. A. Fujimori, T. Araki, H. Nakahara, E. Ito, M. Hara, H. Ishii, Y. Ouchi, and K. Seki, *Chem. Phys. Lett.*, **349**, 6 (2001).
41. Y. Urushihara and T. Nishino, *Langmuir*, **21**, 2614 (2005).
42. Y. Terayama, M. Kobayashi, S. Sasaki, O. Sakata, and A. Takahara, *Trans. Mater. Res. Soc. Jpn.*, **32**, 259 (2007).

